CXCR4 antagonism increases T cell trafficking in the central nervous system and improves survival from West Nile virus encephalitis

Erin E. McCandless*, Bo Zhang†, Michael S. Diamond*†‡, and Robyn S. Klein*†§¶

Departments of *Pathology and Immunology, †Internal Medicine, ‡Molecular Microbiology, and §Anatomy and Neurobiology, Washington University School of Medicine, St. Louis, MO 63110

Edited by Wayne M. Yokoyama, Washington University School of Medicine, St. Louis, MO, and approved June 3, 2008 (received for review January 28, 2008)

The migration of lymphocytes into the CNS during viral encephalitis is hindered by the blood–brain barrier (BBB) such that most infiltrating cells remain localized to perivascular spaces. This sequestration of leukocytes away from the parenchyma is believed to protect the CNS from immunopathologic injury. Infections of the CNS with highly cytopathic neurotropic viruses, such as West Nile virus (WNV), however, require the parenchymal penetration of T lymphocytes for virus clearance and survival, suggesting that perivascular localization might hinder antiviral immune responses during WNV encephalitis. Using human and murine brain specimens from individuals with WNV encephalitis, we evaluated the expression of CXCL12 and its receptor, CXCR4, at the BBB and tested the hypothesis that inhibition of CXCR4 would promote T lymphocyte entry into the CNS parenchyma and increase viral clearance. Antagonism of CXCR4 significantly improved survival from lethal infection through enhanced intraparenchymal migration of WNV-specific CD8$^+$ T cells within the brain, leading to reduced viral loads and, surprisingly, decreased immunopathology at this site. The benefits of enhanced CD8$^+$ T cell infiltration suggest that pharmacologic targeting of CXCR4 may have therapeutic utility for the treatment of acute viral infections of the CNS.

CD8 T cell | CNS | CXCL12 | chemokine | neuropathology

Under normal, uninflamed conditions, the CNS is an immune-privileged site with minimal infiltration by inflammatory cells (1). The limited trafficking of leukocytes is the result of restriction at the blood–brain barrier (BBB); the specialized microvasculature of the CNS that prevents the entry of cells through mechanisms that are incompletely understood. Although immune cell restriction may protect the brain from inappropriate immune activation and neuropathology (2), it may also act as a barrier to successful pathogen clearance during acute infections of the CNS (3). Indeed, one of the hallmarks of viral encephalitis is the development of perivascular infiltrates comprised of virus-specific T cells with minimal invasion of the CNS parenchyma (4). Thus, BBB restriction may limit CNS antiviral immune responses at the expense of delayed clearance of microbial agents.

Studies in mice suggest that polarized expression of the chemokine CXCL12 at the BBB localizes infiltrating mononuclear cells to the perivascular spaces of the CNS microvasculature, therefore limiting their entry into the CNS parenchyma (5). CXCL12 expression is present along the basolateral surfaces of CNS endothelial cells where leukocytes, which ubiquitously express its receptor CXCR4, engage CXCL12 when attempting to enter the CNS. This subcompartment retention, which is analogous to the role of CXCL12 in lymphoid compartments (6), could be an integral component of CNS protection from the pathologic consequences of immune cell activation (7). In CNS autoimmune diseases, such as multiple sclerosis (MS) and its murine model experimental autoimmune encephalomyelitis (EAE), alterations in CXCL12 expression at the BBB contributes to the inappropriate entry of leukocytes, which is associated with significant glial cell activation and CNS injury (5, 8). Whereas immunopathology is an established consequence of CNS lymphocyte entry during noncytopathic viral infections (9), the effects of enhanced lymphocyte migration into the CNS parenchyma during cytopathic viral infections are less clear. Studies of CNS infections with cytopathic viruses, such as West Nile virus (WNV), suggest that lymphocyte presence promotes pathogen clearance but may also lead to immunopathology (10, 11).

To study the role of CXCR4 in regulating lymphocyte trafficking within the CNS during viral encephalitis, we used a well characterized mouse model of WNV encephalitis. WNV, a cytolytic, neurotropic flavivirus that is now endemic in the Northern Hemisphere, causes neuro-invasive disease in the very young, elderly, and immunocompromised, particularly when cell-mediated immunity is impaired. In both humans and mice, WNV targets neurons throughout the CNS, leading to their injury and death (12, 13). Studies in mice indicate that clearance of WNV within the CNS compartment requires the presence of effector CD8$^+$ T cells (14). Thus, the WNV mouse model provides an ideal system in which to determine whether alterations in lymphocyte trafficking into the CNS affects disease outcome. Herein, we show that CXCL12-mediated localization of lymphocytes to the perivascular space modulates their ability to efficiently control infection during WNV encephalitis. Administration of a specific CXCR4 antagonist promoted the intraparenchymal migration of WNV-specific lymphocytes, enhanced viral clearance, and reduced immunopathology within the CNS compartment, leading to significant improvement in survival after WNV infection.

Results

Polarized Expression of CXCL12 at the BBB Restricts Leukocyte Infiltration During WNV Encephalitis. To define the specific roles of CXCL12 and CXCR4 in the neuropathogenesis of WNV encephalitis, we used an established mouse model of acute WNV infection (15). Studies were performed with 5-week-old WT C57BL/6 mice, which have an ≈10% survival rate after s.c. infection with a virulent lineage I New York WNV strain (15). Mice were inoculated with 10 pfu of WNV and examined for brain expression of CXCL12 and CXCR4. Two isoforms of CXCL12 were constitutively expressed in the CNS and have distinct localization and functions: CXCL12α and CXCL12β are expressed by subpopulations of neurons and endothelial cells in the microvasculature, respectively (16). Analysis

Author contributions: E.E.M., M.S.D., and R.S.K. designed research; E.E.M. and B.Z. performed research; E.E.M., B.Z., M.S.D., and R.S.K. analyzed data; and E.E.M., M.S.D., and R.S.K. wrote the paper.

The authors declare no conflict of interest.

This article is a PNAS Direct Submission.

Freely available online through the PNAS open access option.

¶To whom correspondence should be addressed at: Department of Medicine, Washington University School of Medicine, 660 South Euclid Avenue, St. Louis, MO 63110. E-mail: rklein@id.wustl.edu.

This article contains supporting information online at www.pnas.org/cgi/content/full/0800898105/DCSupplemental.

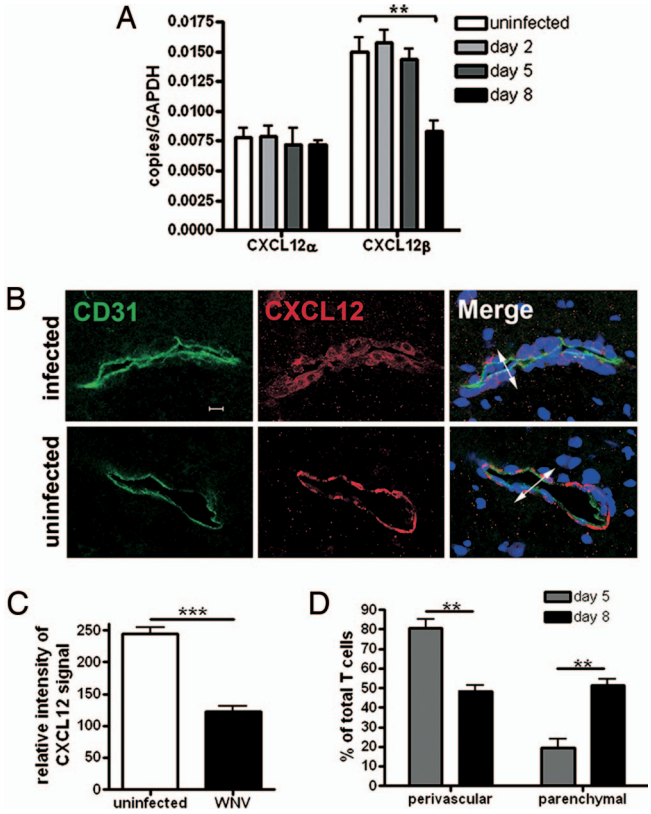

Fig. 1. CXCL12 expression in the CNS during WNV encephalitis. (*A*) QRT-PCR analysis of CXCL12 expression in the CNS of uninfected (white bars) or WNV infected mice (Day 2, light gray bars; Day 5, dark gray bars; and Day 8, black bars). Each group represents at least five individual animals. *, $P < 0.05$; **; $P < 0.005$. (*B*) Confocal immunohistochemical analysis of brain tissue collected from WNV-infected (day 8) (*Upper*) and uninfected (*Lower*) mice. Images were stained for CD31 (green), CXCL12 (red), and nuclei (blue). Representative images are shown for five sections, from three mice, in two separate experiments. IC, isotype control. (Scale bar, 10 μm) (*C*) Relative intensity analysis of CXCL12-stained endothelium in brains of uninfected and WNV-infected (day 8) mice. Data are presented as the average intensity across each vessel for 3–6 mice per group in two separate experiments ±SEM. *, $P < 0.001$. (*D*) Quantitative analyses of perivascular versus parenchymal T cells within brains of WNV-infected mice at days 5 (gray bars) and 8 (black bars) after infection. Data are presented as average percentages of T cells as determined by analyzing the associations of $CD3^+$ cells with respect to CD31-stained vessels and counting the numbers of perivascular versus parenchymal cells in 11–19 low power confocal images for 4–5 mice per group ±SEM. *, $P < 0.001$.

of CXCL12α and β mRNA levels from uninfected and WNV-infected mice at various days after infection revealed a change in expression of only the β isoform, which was significantly decreased ($P = 0.004$) by day 8 (Fig. 1*A*).

Consistent with the RNA analyses, evaluation of CXCL12 protein expression within the brain microvasculature via confocal microscopy revealed a decrease in the intensity of staining in WNV-infected mice compared with uninfected controls (Fig. 1*B*). Semiquantitative analysis of confocal images revealed that the level of CXCL12 protein expression at the BBB was decreased by ≈50% compared with that observed within the brain microvessels of uninfected mice (Fig. 1*C*), and CXCL12 was detected only on basolateral surfaces of the endothelium [supporting information (SI) Fig. S1]. Similarly, examination of CXCL12 expression in human brain tissue from two individuals with WNV encephalitis revealed CXCL12 expression at basolateral endothelium surfaces only (Fig. S2*A*). To determine whether decreased expression of CXCL12 at the BBB affected the intraparenchymal trafficking of T cells, we examined the relative positions of $CD3^+$ cells with respect to the $CD31^+$ microvasculature via double-label immunohistochemical analyses of brains from mice at days 5 and 8 after infection with WNV. Consistent with the CXCL12 expression data, percentages of perivascular T cells were significantly lower, and parenchymal T cells were significantly higher at day 8 after infection (Fig. 1*D*).

Prior studies have demonstrated that leukocytes begin to infiltrate the CNS of WNV-infected mice at ≈1 week after infection (17). Despite the significant decrease in CXCL12 expression at this time-point, the brain microvasculature in mice with WNV encephalitis displayed perivascular infiltrates because few leukocytes entered into the parenchyma at day 8 after infection (Fig. 2*A*). The vast majority of infiltrating $CD45^+$ perivascular leukocytes strongly expressed CXCR4 (Fig. 2*A Left* and *Right*). Detection of a ligand-induced, phosphorylated form of CXCR4 (pCXCR4) with phospho-serine^{339}-CXCR4-specific antibodies (18) demonstrated that pCXCR4 was present only in a subpopulation of leukocytes within perivascular spaces. In contrast, leukocytes present in the vessel lumina were negative for the phosphorylated form of CXCR4 (Fig. 2*A Center*). These data suggest that CXCR4-expressing leukocytes are not activated by CXCL12 until they enter the perivascular space. Consistent with the entry of CXCR4-expressing infiltrating leukocytes into the CNS, levels of CXCR4 mRNA within the brains of mice with WNV encephalitis were increased 4-fold at day 8 after infection, (Fig. 2*B*) with no change seen at days 2 or 5. Flow cytometric analysis of the cells isolated from the brains of mice with WNV encephalitis revealed that these $CXCR4^+$ cells were primarily $CD11b^+$ macrophages/microglia and $CD8^+$ T cells with few, if any, $CD4^+$ T helper cells (Fig. 2*C*). Human CXCR4 staining showed a similar pattern of expression on leukocytes within perivascular infiltrates (Fig. S2*B*). The expression patterns of CXCL12β and CXCR4 in the CNS suggest that these molecules regulate the trafficking of leukocytes into the perivascular space during WNV in both human and murine disease.

CXCR4 Antagonism Increases Survival and Decreases Brain Viral Burden After WNV Infection. Given the predominance of CXCR4 expression on perivascular T cells in both murine and human brain during WNV encephalitis, we hypothesized that the CXCL12-CXCR4-mediated localization prevented migration by retaining cells in the perivascular space. Accordingly, disruption of this localization might promote migration of WNV-specific T cells into the CNS parenchyma and enhance recovery from WNV encephalitis. To test this, we treated 5-week-old C57BL/6 mice with the CXCR4 antagonist AMD3100, which specifically blocks binding of CXCL12 to CXCR4 (19). To ensure sufficient levels of the antagonist throughout the 16-day experimental period, AMD3100 was delivered via a s.c. osmotic infusion pump. Continuous administration of AMD3100, beginning at the time of infection, increased ($P = 0.006$) survival of WNV-infected animals to 50% compared with infected mice that received vehicle (PBS) alone (Fig. 3*A*). Animals from both treatment groups showed clinical signs of infection including weight loss, hunching, fur ruffling, and decreased activity, although ≈50% of the mice treated with AMD3100 showed clinical improvement by day 8, whereas the PBS-treated mice continued to sicken until death.

Virologic analysis after treatment with AMD3100 revealed no differences in splenic viral burdens throughout the time course or brain viral burdens through day 6 between the two treatment groups (Fig. 3*B*). However, by day 8, AMD3100-treated animals showed an ≈1,000-fold decrease in infectious virus within the brain compared with PBS-treated controls ($P = 0.0002$) (Fig. 3*C*). Thus, CXCR4 inhibition increased the survival of mice with WNV encephalitis and promoted viral clearance, specifically within the brain. Attempts at continuous dosing begun 4 days after exposure were unsuccessful because the combined stress of surgery and WNV neuroinvasion led to excessive mortality. Thus, therapeutic administration of AMD3100 by an i.p. route was attempted.

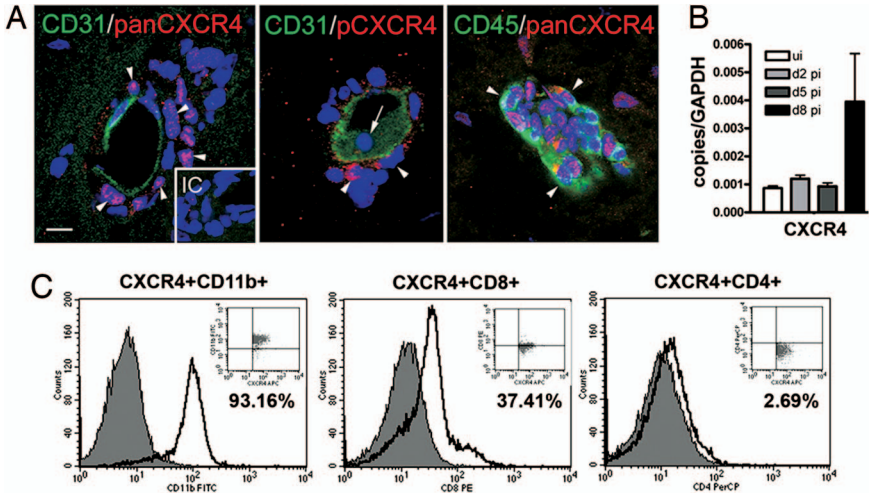

Fig. 2. CXCR4 expression and activation in the CNS during WNV encephalitis. (*A*) Sections from WNV-infected brain at day 8 after infection were stained for CD31 (green) and pan-CXCR4 (red) (*Left*), pCXCR4 (red) (*Center*), or CD45 (green) and pan-CXCR4 (red) (*Right*). Pan- and pCXCR4-labeling of perivascular cells are shown with arrowheads (*Left* and *Center*), pCXCR4-negative luminal cells are shown with an arrow (*Center*), and perivascular cells are exclusively leukocytes, shown with arrowheads (*Right*). Representative images shown are of 10 sections, from three mice, from two independent experiments. IC, isotype control. (Scale bar, 10 μm) (*B*) QRT-PCR analysis of CXCR4 mRNA levels in brain tissue from uninfected (white bars) and WNV-infected mice at day 2 (light gray bars), 5 (dark gray bars), and 8 (black bars). $n = 5$ animals per group. (*C*) Flow cytometric analysis of CNS leukocytes at day 8 after infection through a CXCR4$^+$ gate and immunophenotyped for CD11b$^+$ (*Left*), CD8$^+$ (*Center*), and CD4$^+$ (*Right*). $n = 2$ experiments with 10 mice per group.

Interval dosing of AMD3100 was difficult because of a maximum plasma half-life of only 0.9 h in rodents (20) (<6% remaining in plasma by 4 h after administration). Nonetheless, twice daily dosing of AMD3100 beginning at day 4 after infection still significantly prolonged survival (mean time to death of PBS and AMD3100 mice was 9.6 and 11.0 days, respectively, $P = 0.02$), although no overall survival benefit was observed (Fig. S3).

CXCR4 Antagonism Enhances T Cell Penetration in the Brain After WNV Encephalitis. To assess whether CXCR4 antagonism affected the intraparenchymal migration of mononuclear cells, we performed flow cytometric analysis of leukocytes isolated from the brains of AMD3100- and PBS-treated mice. On day 6 after WNV infection, when immune cells begin to migrate into the brain (17), equivalent numbers of leukocytes were observed in the brains of both groups of animals (Fig. 4*A Left*). However, by day 8 after infection, the number of brain leukocytes of PBS-treated mice had doubled, whereas in AMD3100-treated mice, the leukocyte numbers had declined ($P < 0.05$) (Fig. 4*A Center* and *Right*). There was no difference in the numbers of CD8$^+$ or CD4$^+$ T cells at day 6 or 8 after infection within the brains of AMD3100-treated mice compared with PBS-treated controls after WNV infection (Fig. 4*B Center* and *Right*). Instead, higher numbers (3.5-fold increase, $P = 0.007$) of CD11b$^+$ macrophages/microglia were detected in the brains of PBS-treated mice, accounting for the overall increase in cell number (Fig. 4*B Left*). Because we speculated that the equivalent number of T cells in AMD3100-treated mice might localize to sites of infection and thus be more functionally relevant, we evaluated the penetration of CD3$^+$ cells into the brain parenchyma of WNV-infected PBS- and AMD3100-treated mice. Although inflammation was present in infected mice of both treatment groups, T cells within brain tissues of PBS-treated mice were

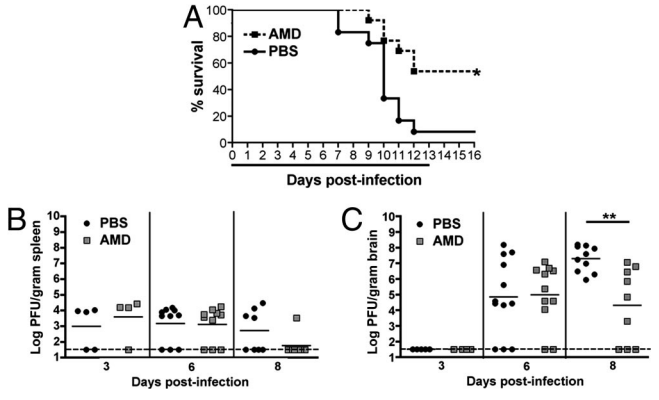

Fig. 3. Antagonism of CXCR4 and WNV infection. (*A*) C57BL/6 mice were infected with 10 pfu of WNV and treated with vehicle only ($n = 12$) or AMD3100 at 142 μg/day ($n = 13$) via continuous dosing by s.c. osmotic pumps during days 0 to 13 after infection, as indicated by the black line, in two independent experiments. (*B* and *C*) Analysis of viral burden in splenic (*B*) and brain (*C*) tissues of PBS- (black circles) or AMD3100- (gray squares) treated mice over the time course of infection. Data are from two independent experiments. *, $P < 0.05$; **, $P < 0.005$.

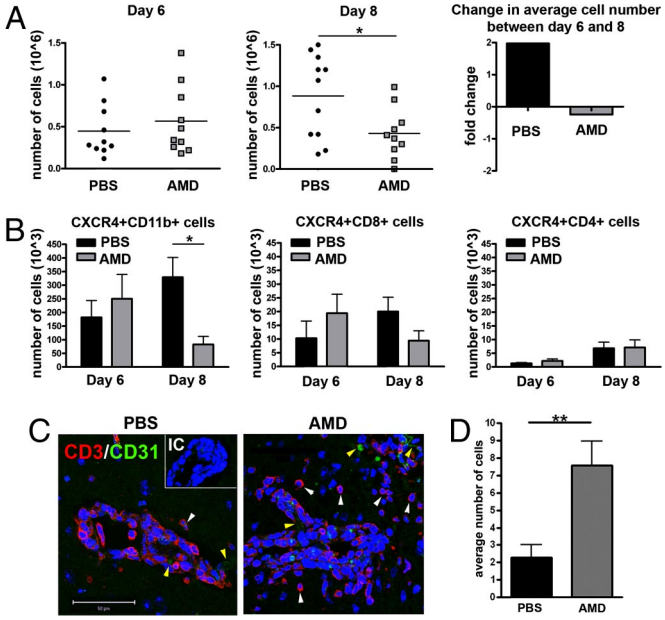

Fig. 4. CXCR4 antagonism promotes intraparenchymal migration of T cells within the brains of WNV-infected mice. (*A*) Total numbers of leukocytes isolated per brain from PBS- (black circles) and AMD3100- (gray squares) treated mice on days 6 (*Left*) and 8 (*Center*) after infection from two independent experiments. (*Right*) Indicates the fold-change in average cell number of PBS- (black bar) or AMD3100- (gray bar) treated mice between days 6 and 8. (*B*) Total numbers of CXCR4$^+$ leukocytes isolated per brain (CD11b$^+$, CD8$^+$, and CD4$^+$) from PBS- (black bars) or AMD3100- (gray bars) treated mice. Data reflects two independent experiments. $n = 9$–11 animals per group; *, $P < 0.05$. (*C*) Brain sections from PBS- (*Left*) and AMD3100- (*Right*) treated animals at day 6 after infection were stained for CD31 (green), CD3 (red), and nuclei (blue) and visualized at high power. Representative images shown from at least three mice. IC, isotype control. (Scale bar, 50 μm) (*D*) Quantitation of average number of parenchymal T cells per high power field, as determined by a blinded observer. Shown are 18 images from two AMD3100-treated mice and 14 images from three PBS-treated mice. *, $P < 0.05$.

primarily sequestered within the perivascular spaces whereas T cells in AMD3100-treated mice had migrated extensively into the tissue parenchyma at day 6 after infection (Fig. 4*C*). Quantitative analyses of the positioning of $CD3^+$ cells, with respect to the $CD31^+$ endothelium, revealed a significant (3.4-fold, $P = 0.003$) increase in the numbers of intraparenchymal $CD3^+$ cells within the brains of AMD3100-treated mice (Fig. 4*D*). Analysis of $CD3^+$ cells within the brains of human patients with WNV encephalitis also demonstrated minimal parenchymal infiltration similar to that observed in PBS-treated mice (Fig. S2*C*).

To determine whether the effect of AMD3100 was specific to CNS migration of leukocytes, we performed a similar analysis of splenic tissue obtained from WNV-infected mice at various days after infection. AMD3100 treatment had no effect ($P = 0.2$ and 0.7) on total splenocyte numbers at days 3 and 6 after infection (Fig. S4*A*) or in the number of $CXCR4^+CD11b^+$, $CXCR4^+CD8^+$, and $CXCR4^+CD4^+$ cells collected at days 3, 6, and 8 after infection (Fig. S4*B*). There were, however, significantly fewer (2.3-fold, $P = 0.01$) total splenocytes (Fig. S4*A*) in the PBS-treated mice at day 8 after infection, which is consistent with the severe involution of the spleen that occurs in animals that succumb to WNV infection (21).

Antagonism of CXCR4 Promotes $CD8^+$ T Cells Access to Virally Infected Cells. The increased parenchymal migration and decreased viral loads observed in the brains of AMD3100-treated mice with WNV encephalitis suggested that antagonism of CXCR4 may function to increase encounters between WNV-specific $CD8^+$ T cells and virally infected target cells. To evaluate this, we analyzed T cell proximity to WNV-infected neurons via double-label, confocal microscopy at day 6 after infection, when absolute viral loads and numbers of brain infiltrating cells were equivalent between the treatment groups. In AMD3100-treated mice, T cells were dispersed throughout the parenchyma and in close proximity to areas with a high density of WNV-infected cells (Fig. 5*A Right*). In contrast, in PBS-treated mice, T cells were retained in perivascular spaces and generally not present at the site of viral infection in the parenchyma (Fig. 5*A Left*). The $CD8^+$ T cells isolated from the CNS tissues of AMD3100-treated mice at day 6 after infection were antigen-specific because they produced IFN-γ after *ex vivo* stimulation with an immunodominant D^b-restricted NS4B peptide (22). Consistent with this finding, higher levels of antigen-specific T cells were observed in AMD3100-treated compared with PBS-treated animals (1.9-fold increase, $P = 0.01$) (Fig. 5 *B* and *C*). No difference in IFN-γ levels after *ex vivo* stimulation was observed in splenic $CD8^+$ T cells from PBS-and AMD3100-treated mice, indicating that AMD3100 does not affect WNV-specific $CD8^+$ T cells in the periphery (Fig. 5*C*). These experiments suggest that CXCR4 antagonism increases the efficiency of T cell migration into the brain parenchyma, which enhances the encounter of WNV-specific $CD8^+$ T cells with infected target cells, resulting in a more rapid viral clearance.

CXCR4 Antagonism Is also Associated with Decreased Glial Cell Activation Within the WNV-Infected Brain. Infiltrating leukocytes activate resident glial cells, often with deleterious and pathological consequences (7). To determine whether efficient viral clearance in the setting of CXCR4 antagonism altered immunopathology, we examined astrocyte and microglial activation at day 8 after infection; a time point at which dying, PBS-treated mice continue to develop immune cell infiltrates, and AMD3100-treated mice are recovering (Fig. 6). GFAP, a marker for activated astrocytes, was widely expressed in PBS- treated mice, whereas very little GFAP expression was detected in AMD3100-treated mice (Fig. 6*A*). The significant increase (2.4-fold, $P = 0.04$) in total area of astrocyte activation (Fig. 6*B*) coincided with the presence of $CD3^+$ T cells (Fig. 6*A*). Additionally, increases in microglia activation were observed even in the absence of extensive $CD3^+$ T cell infiltration (Fig. 6*C*). Flow cytometric analysis revealed that although the total

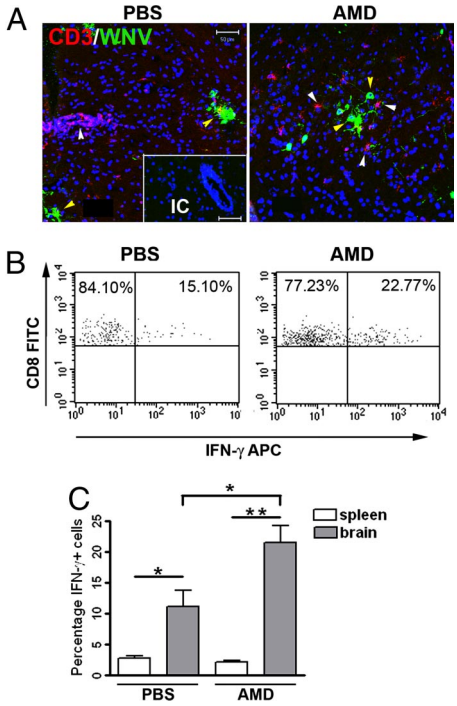

Fig. 5. Effect of CXCR4 antagonism on T cell entry and activation in the CNS. CNS tissue from WNV-infected animals treated with PBS or AMD3100 were collected at day 6, when total cell numbers where the same from both groups. (*A*) Confocal immunohistochemical analysis shows location of $CD3^+$ cells relative to WNV infected neurons. Brain sections from PBS- (*Left*) and AMD3100- (*Right*) treated animals were stained for WNV antigen (green), CD3 (red), and nuclei (blue). All images were collected by using identical laser settings to allow for direct intensity comparison. Representative images from at least three mice shown. IC, isotype control.(Scale bar, 50 μm) (*B*) $CD8^+$ T cells isolated from the CNS of PBS- (*Left*) and AMD3100- (*Right*) treated mice were restimulated *ex vivo* with an NS4B WNV peptide before measurement of IFN-γ production. Representative flow cytometry dot plots depict stained cells shown through a $CD8^+$ T cell gate. (*C*) Quantification by flow cytometry of NS4B-specific $CD8^+$ cells isolated from spleens and CNS of PBS- (black bars) or AMD3100- (gray bars) treated mice. $n = 11$ animals per group. Data shown represents two independent experiments. *, $P < 0.05$.

numbers of resting microglia were identical between mice with WNV encephalitis in both treatment groups, there was a trend toward an increase ($P = 0.07$) in macrophages and a significant increase (6.8-fold, $P = 0.03$) in activated microglia in the PBS-treated animals at day 8 after infection (Fig. 6*D*). Thus, antagonism of CXCR4 may additionally promote recovery by minimizing pathologic immune activation that occurs during viral encephalitis.

Discussion

The goal of an effective antiviral immune response is to clear pathogens without causing undue tissue injury. In the brain, which has little reserve for damage, the BBB serves to dampen immune activation by preventing the entry of leukocytes, whose presence within the CNS parenchyma are believed to be universally detrimental by inducing excessive glial cell activation (7). Our data indicate that the opposite is true during CXCR4 antagonism, in the setting of WNV encephalitis, offering insights into the consequences of virus-specific T lymphocyte entry during cytopathic viral infections. We showed that the restricted entry of T lymphocytes at the BBB, which is mediated by CXCL12 and its receptor CXCR4, prevents virus-specific $CD8^+$ T cells from clearing WNV within the CNS parenchyma. CXCR4 antagonism, which released these cells from their sequestration within perivascular spaces, led to increased encounters with virus-infected targets within the brain parenchyma and enhanced viral clearance. The increased efficiency of this

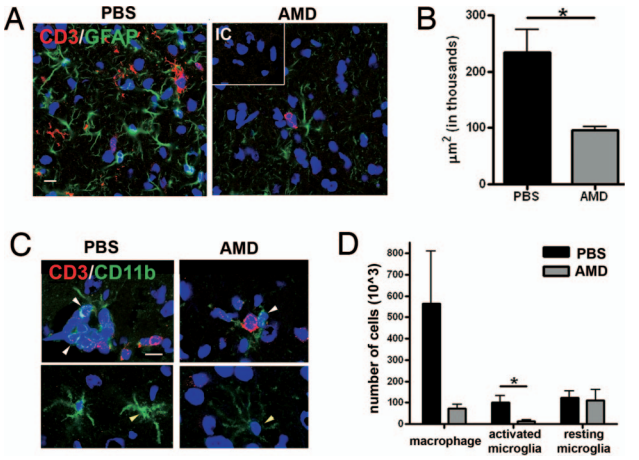

Fig. 6. Analysis of glial activation during CXCR4 antagonism. Brain tissues from WNV-infected, PBS- and AMD3100-treated mice were collected on day 8, when the former group continues to worsen whereas the latter group is recovering. (*A*) Confocal analysis of GFAP (green) and CD3 (red) expression in brain sections from PBS- (*Left*) or AMD3100- treated mice (*Right*). Nuclei are counterstained (blue). IC, isotype control. (Scale bar, 10 μm) Representative images shown are from 2–3 mice per group and 6–9 images per mouse. (*B*) Volocity™ image analysis software was used to quantitate GFAP staining in PBS- (black bars) and AMD3100- (gray bars) treated mice with WNV encephalitis. $n = 4$. Representative images are taken from two mice. (*C*) Double-labeling of CNS sections from PBS- (*Left*) or AMD3100-treated mice (*Right*) for CD11b (green), CD3 (red), and nuclei (blue). Yellow arrowheads indicate microglial and white arrowheads indicate macrophages. Representative images shown are from 2–3 mice per group and 3–6 images per mouse. (*D*) Flow cytometric quantitation of total numbers of macrophages ($CD45^{high}CD11b^{high}$) and resting ($CD45^{low}CD11b^{low}$) or activated ($CD45^{high}CD11b^{low}$) microglia from CNS of PBS- (black bars) and AMD3100- (gray bars) treated mice at day 8 after infection with WNV. $n = 7$–8 animals per group for two experiments. *, $P < 0.05$.

process limited the extent of immunopathology and enhanced survival. These data therefore provide evidence that the parenchymal location of virus-specific T cells is essential for the effective clearance of WNV within the CNS, which minimize glial cell activation.

$CD8^+$ T cell migration into the CNS is required for clearance of a variety of neurotropic viruses, including mouse hepatitis virus (23), WNV (17), lymphocytic choriomeningitis virus (24), Japanese encephalitis virus (25), and measles virus (26). T cell control of an acute cytopathic viral infection in the CNS, however, may be offset by direct and/or bystander damage from cytotoxic effects. Indeed, infection with less cytopathic lineage II strains of WNV results in extensive $CD8^+$ T cell-mediated neuronal injury and death (27). Virus-specific versus bystander $CD8^+$ T cell infiltration could differentially activate glial cells and lead to neuronal injury (7). As expression of CXCR4 is induced on murine cytotoxic $CD8^+$ T cells after *in vivo* activation (28), CXCR4 antagonism may preferentially induce the migration of virus-specific CD8 T cells. Glial activation, however, may also be triggered by specific T cell subsets or antigen targets because AMD3100-treated mice with EAE display increases in both intraparenchymal T cell migration and in numbers of activated microglia (5).

Our data also suggest that the homeostatic function of CXCL12 in preventing leukocyte egress at the BBB may be maladaptive in the setting of WNV infection. Although down-regulation of the endothelial cell-specific isoform CXCL12β might occur during inflammatory responses that require parenchymal penetration of immune cells (16), this is apparently insufficient to allow efficient T cell trafficking during WNV encephalitis. In contrast, redistribution of CXCL12 across the endothelium has been observed to occur during CD4 T cell-mediated CNS autoimmune diseases. Thus, during experimental EAE (5) and MS (8), CXCL12 is no longer concentrated within the perivascular space, and CXCR4-expressing CD4 T cells readily enter the parenchyma and induce inflammatory demyelination. The mechanisms that regulate CXCL12 expression at the BBB are unknown but may relate to factors expressed by infiltrating immune cells. Thus, contrary to the role of CXCL12 within secondary lymphoid tissues (29), the movement of leukocytes into and out of CNS perivascular spaces relies on regulation of ligand expression and/or location rather than at the chemokine receptor level. Future studies using tissue-specific transgenic approaches are needed to further define *in vivo* roles of CXCL12 and CXCR4 at the BBB during WNV and other viral encephalitides.

Outside the CNS, CXCR4 is ubiquitously expressed on leukocytes and coordinates their trafficking within secondary lymphoid tissue (30). Decreased responsiveness to CXCL12 and surface expression of CXCR4 occurs during the evolution of antiviral immune responses, allowing proper egress of leukocytes that participate in pathogen clearance (31). Consistent with these findings, we did not see alterations in T cell trafficking, virus-specific immune responses, or viral clearance within the spleens of WNV-infected mice treated with AMD3100, compared with similarly infected, vehicle-treated animals. In disease models in which CXCL12 acts in a homeostatic function to localize leukocytes to endothelium, CXCR4 antagonism leads to increased tissue inflammation (5, 32). Our data demonstrating that CXCR4 antagonism promotes parenchymal CD8 T cell infiltration into the brain therefore supports its homeostatic role at this tissue site.

Based on our studies, CXCR4 antagonists may be expected to expedite viral clearance in acute viral encephalitides that require influx of protective lymphocytes. Thus, regulation of leukocyte infiltration may be a therapeutic strategy for control of CNS viruses, many of which lack specific treatments. Indeed, in a murine model of rabies encephalitis, administration of a sex steroid enhanced BBB permeability, promoted immune cell penetration into the CNS, and improved survival (33). These studies and our data suggest that ineffective pathogen clearance during viral infections of the CNS parenchyma may be the result of BBB restraint, which hinders immune responses specifically within the CNS. Immunotherapy with CXCR4 antagonists alone or in combination with antiviral modalities (34) might enhance clearance within the CNS in potentially fatal viral infections.

Resolution of CNS infection is often a balance between immune-mediated pathogen clearance and the deleterious effects of inflammation. We have shown that CXCL12 localizes lymphocytes within CNS perivascular spaces in both humans and mice with WNV encephalitis. Our work illustrates that manipulation of the immune response by the use of chemokine receptor antagonists can promote an early increase in immune cell trafficking that controls viral infection, ultimately leading to a rapid dampening of inflammation that can have pathologic consequences.

Materials and Methods

Mouse Model of WNV Infection. Five-week-old male C57BL/6 mice (Jackson Laboratories) were used for all experiments. Mice were maintained under pathogen-free conditions (Department of Comparative Medicine, Washington University), and studies were performed in compliance with the guidelines of the Washington University School of Medicine Animal Safety Committee. The WNV strain 3000.0259 was isolated in New York in 2000 and passaged as described (35). Anesthetized mice were infected via footpad with 10 pfu of WNV as described (15). Immunohistochemical and virological analyses of WNV-infected tissues were performed as described (5, 15).

Quantitative RT-PCR. Total RNA and quantitative RT-PCR (QRT-PCR) was performed by using primers generated with Primer Express 2.0 software (Applied Biosystems) for CXCL12 isoforms and CXCR4, as published (5).

Antibodies. The following antibodies were used in this study: CXCL12 rabbit polyclonal (Peprotech), IgG isotype (Jackson ImmunoResearch), CXCR4 polyclonal (panCXCR4, Leinco), monoclonal rat anti-mouse-CD31 (PECAM) (BD

Pharmingen), anti-CD11b (BD PharMingen), anti-CD3 (Dako), and anti- GFAP (Invitrogen) antibodies; WNV antigen immune rat serum (12); and fluorescently conjugated antibodies against CD4, CD8, CD11b, CXCR4, and IFN-γ (BD PharMingen). Phosphoserine 339-CXCR4 specific antibodies (pCXCR4) have been described (18).

Immunohistochemistry. Frozen sections were prepared from animals perfused with PBS as described (5). Detection of CXCL12, CD3 and anti-CD31 (PECAM), and CXCR4 with panCXCR4 and pCXCR4 antibodies was performed as described (5, 18). Primary antibodies were detected with goat anti-rabbit or anti-rat IgG conjugated to Alexa 555 or Alexa 488 (Molecular Probes), and nuclei were counterstained with ToPro3. Sections were analyzed by using a Zeiss LSM 510 laser scanning confocal microscope and accompanying software (Zeiss). Quantitative analyses of parenchymal T cells was performed in a blinded fashion by counting the numbers of $CD3^+$ cells that were not associated with $CD31^+$ microvasculature, per high power field.

Flow Cytometry. Cells were isolated from WNV-infected mouse tissues as described (36) and stained with fluorescently conjugated antibodies to CD4, CD8, CD11b, CXCR4, and IFN-γ. Data collection and analysis were conducted with a FACScalibur™ flow cytometer by using CellQuest™ software (Becton Dickinson), as described (5). Differentiation between infiltrating macrophages and microglia in WNV-infected brain tissues was accomplished via comparisons between levels of CD45 and CD11b staining, as described (5).

***In Vivo* AMD3100 Treatment.** Continuous dose treatment with AMD3100 or PBS was achieved by using 14-day osmotic pumps with an infusion rate of 0.5 μl/h (Alzet), as described (5). Osmotic pumps were implanted s.c. at the time of WNV infection. For experiments performed after exposure, 100 μg of AMD3100 in sterile PBS or PBS alone was administered i.p. every 12 h.

Peptide Restimulation of T Cells. Leukocytes were isolated from brains and spleens from WNV-infected mice on day 6 after infection, stimulated with an immunodominant D^b-restricted NS4B WNV peptide, and stained for IFN-γ, as described (22) (see *Human CNS Tissues* in *SI Text*).

Statistical Analysis. Data were analyzed by using Prism software (GraphPad). The Student's *t* test was used to determine the statistical significance of QRT-PCR, histological, and flow cytometry analyses. For survival experiments, Kaplan–Meier survival curves were analyzed by the log-rank test. For virus burden experiments, statistical significance was determined via the Mann–Whitney test. In all experiments, $P < 0.05$ was considered to be significant.

ACKNOWLEDGMENTS. The authors thank Dr. J. Rubin (Washington University) for the phospho-serine339-CXCR4 antibodies; Dr. Levy (St. Louis University, St. Louis) for human WNV tissues; Drs. J. Russell, D. Goldberg, and H. Virgin for their critical reviews of the manuscript; and J. Sim, M. Engle, D. Koch, and M. Krause for technical assistance. The work was supported by National Institutes of Health/National Institute of Neurological Disorders and Stroke Grants NS045607 and NS052632 and by a grant from the Midwest Regional Center for Excellence in Emerging Infectious Diseases.

1. Ransohoff RM, Kivisakk P, Kidd G (2003) Three or more routes for leukocyte migration into the central nervous system. *Nat Rev Immunol* 3:569–581.
2. McGavern DB, Truong P (2004) Rebuilding an immune-mediated central nervous system disease: Weighing the pathogenicity of antigen-specific versus bystander T cells. *J Immunol* 173:4779–4790.
3. Hausmann J, *et al.* (2005) CD8 T cells require gamma interferon to clear borna disease virus from the brain and prevent immune system-mediated neuronal damage. *J Virol* 79:13509–13518.
4. Bouffard JP, Riudavets MA, Holman R, Rushing EJ (2004) Neuropathology of the brain and spinal cord in human West Nile virus infection. *Clin Neuropathol* 23:59–61.
5. McCandless EE, Wang Q, Woerner BM, Harper JM, Klein RS (2006) CXCL12 limits inflammation by localizing mononuclear infiltrates to the perivascular space during experimental autoimmune encephalomyelitis. *J Immunol* 177:8053–8064.
6. Bleul CC, Schultze JL, Springer TA (1998) B lymphocyte chemotaxis regulated in association with microanatomic localization, differentiation state, and B cell receptor engagement. *J Exp Med* 187:753–762.
7. Dheen ST, Kaur C, Ling EA (2007) Microglial activation and its implications in the brain diseases. *Curr Med Chem* 14:1189–1197.
8. McCandless EE, *et al.* (2008) Pathologic expression of CXCL12 at the blood brain barrier correlates with severity of Multiple Sclerosis. *Am J Pathol* 172:799–808.
9. Rempel JD, Murray SJ, Meisner J, Buchmeier MJ (2004) Mouse hepatitis virus neurovirulence: Evidence of a linkage between S glycoprotein expression and immunopathology. *Virology* 318:45–54.
10. King NJ, *et al.* (2007) Immunopathology of flavivirus infections. *Immunol Cell Biol* 85:33–42.
11. Wang Y, Lobigs M, Lee E, Mullbacher A (2003) $CD8^+$ T cells mediate recovery and immunopathology in West Nile virus encephalitis. *J Virol* 77:13323–13334.
12. Shrestha B, Gottlieb D, Diamond MS (2003) Infection and injury of neurons by West Nile encephalitis virus. *J Virol* 77:13203–13213.
13. Kleinschmidt-DeMasters BK, *et al.* (2004) Naturally acquired West Nile virus encephalomyelitis in transplant recipients: Clinical, laboratory, diagnostic, and neuropathological features. *Arch Neurol* 61:1210–1220.
14. Shrestha B, Samuel MA, Diamond MS (2006) $CD8^+$ T cells require perforin to clear West Nile virus from infected neurons. *J Virol* 80:119–129.
15. Engle MJ, Diamond MS (2003) Antibody prophylaxis and therapy against West Nile virus infection in wild-type and immunodeficient mice. *J Virol* 77:12941–12949.
16. Stumm RK, *et al.* (2002) A dual role for the SDF-1/CXCR4 chemokine receptor system in adult brain: Isoform-selective regulation of SDF-1 expression modulates CXCR4-dependent neuronal plasticity and cerebral leukocyte recruitment after focal ischemia. *J Neurosci* 22:5865–5878.
17. Shrestha B, Diamond MS (2004) Role of $CD8^+$ T cells in control of West Nile virus infection. *J Virol* 78:8312–8321.
18. Woerner BM, Warrington NM, Kung AL, Perry A, Rubin JB (2005) Widespread CXCR4 activation in astrocytomas revealed by phospho-CXCR4-specific antibodies. *Cancer Res* 65:11392–11399.
19. Hatse S, Princen K, Bridger G, De Clercq E, Schols D (2002) Chemokine receptor inhibition by AMD3100 is strictly confined to CXCR4. *FEBS Lett* 527:255–262.
20. Datema R, *et al.* (1996) Antiviral efficacy in vivo of the anti-human immunodeficiency virus bicyclam SDZ SID 791 (JM 3100), an inhibitor of infectious cell entry. *Antimicrob Agents Chemother* 40:750–754.
21. Ben-Nathan D, *et al.* (1992) Dehydroepiandrosterone protects mice inoculated with West Nile virus and exposed to cold stress. *J Med Virol* 38:159–166.
22. Purtha WE, *et al.* (2007) Antigen-specific cytotoxic T lymphocytes protect against lethal West Nile virus encephalitis. *Eur J Immunol* 37:1845–1854.
23. Glass WG, Chen BP, Liu MT, Lane TE (2002) Mouse hepatitis virus infection of the central nervous system: Chemokine-mediated regulation of host defense and disease. *Viral Immunol* 15:261–272.
24. Lauterbach H, Zuniga EI, Truong P, Oldstone MB, McGavern DB (2006) Adoptive immunotherapy induces CNS dendritic cell recruitment and antigen presentation during clearance of a persistent viral infection. *J Exp Med* 203:1963–1975.
25. Murali-Krishna K, Ravi V, Manjunath R (1996) Protection of adult but not newborn mice against lethal intracerebral challenge with Japanese encephalitis virus by adoptively transferred virus-specific cytotoxic T lymphocytes: Requirement for $L3T4^+$ T cells. *J Gen Virol* 77(4):705–714.
26. Tishon A, *et al.* (2006) CD4 T cell control primary measles virus infection of the CNS: Regulation is dependent on combined activity with either CD8 T cells or with B cells: CD4, CD8, or B cells alone are ineffective. *Virology* 347:234–245.
27. Wang T, *et al.* (2003) IFN-gamma-producing gamma delta T cells help control murine West Nile virus infection. *J Immunol* 171:2524–2531.
28. Schabath R, *et al.* (1999) The murine chemokine receptor CXCR4 is tightly regulated during T cell development and activation. *J Leukoc Biol* 66:996–1004.
29. Wehrli N, *et al.* (2001) Changing responsiveness to chemokines allows medullary plasmablasts to leave lymph nodes. *Eur J Immunol* 31:609–616.
30. Chiba K, Matsuyuki H, Maeda Y, Sugahara K (2006) Role of sphingosine 1-phosphate receptor type 1 in lymphocyte egress from secondary lymphoid tissues and thymus. *Cell Mol Immunol* 3:11–19.
31. Kobayashi N, Takata H, Yokota S, Takiguchi M (2004) Down-regulation of CXCR4 expression on human $CD8^+$ T cells during peripheral differentiation. *Eur J Immunol* 34:3370–3378.
32. Aboumrad E, Madec AM, Thivolet C (2007) The CXCR4/CXCL12 (SDF-1) signalling pathway protects non-obese diabetic mouse from autoimmune diabetes. *Clin Exp Immunol* 148:432–439.
33. Roy A, Hooper DC (2007) Lethal silver-haired bat rabies virus infection can be prevented by opening the blood-brain barrier. *J Virol* 81:7993–7998.
34. Morrey JD, *et al.* (2006) Humanized monoclonal antibody against West Nile virus envelope protein administered after neuronal infection protects against lethal encephalitis in hamsters. *J Infect Dis* 194:1300–1308.
35. Ebel GD, *et al.* (2001) Partial genetic characterization of West Nile virus strains, New York State, 2000. *Emerg Infect Dis* 7:650–653.
36. Klein RS, *et al.* (2005) Neuronal CXCL10 directs $CD8^+$ T-cell recruitment and control of West Nile virus encephalitis. *J Virol* 79:11457–11466.